Transverse instabilities in photorefractive counterpropagating two-wave mixing

O. Sandfuchs, J. Leonardy, and F. Kaiser

Institute of Applied Physics, Darmstadt University of Technology, Hochschulstrasse 4a, 64289 Darmstadt, Germany

M. R. Belić

Institute of Physics, P.O. Box 57, 11001 Belgrade, Yugoslavia

Received November 18, 1996

Threshold analysis for transverse instabilities in photorefractive counterpropagating two-wave mixing through reflection gratings is performed. A numerical algorithm for the treatment of wave equations in this geometry is developed, displaying the emergence of running transverse waves. They appear above a threshold in the applied electric field, and their transverse wave number and oscillation frequency agree well with the values predicted by stability analysis. © 1997 Optical Society of America

Following the pioneering work by Honda[1] on the formation of transverse wave patterns in photorefractive (PR) media, a number of reports[2,3] appeared, aimed at explaining the phenomenon. In a geometry of two counterpropagating beams, transverse oscillatory instabilities arise, leading to the generation of sidebands and the formation of hexagonal patterns. Explanation is impeded by the fact that the patterns appear through reflection gratings, which is known to cause difficulties for analytical and numerical treatment. Threshold analyses performed thus far[2,3] offer improved understanding; however, significant differences persist. We attempt to improve the analyses by including two important missing ingredients.

The first ingredient is taking into account temporal variations in the grating amplitude Q when performing stability analysis. In sluggish PR media the variations in Q are driving the secondary instability directly and should be included in the analysis. The second ingredient is taking into account strong modulation depth effects. Up to now the dispersion relations were derived in the limit of high fringe visibility, whereas the wave equations came from the Kukhtarev model, valid for shallow modulation. Based on these improvements a transverse numerical procedure is formulated, displaying the appearance of secondary instabilities—the running transverse waves.

The starting point is the scaled equations in the slowly varying envelope approximation for the PR two-wave mixing through reflection gratings,[4]

$$\partial_z A_1 + i\phi\,\partial_x{}^2 A_1 = -QA_2\,, \tag{1a}$$

$$-\partial_z A_2 + i\phi\,\partial_x{}^2 A_2 = Q^* A_1\,, \tag{1b}$$

where A_1 and A_2 are the forward- and backward-propagating beams, respectively, and ϕ is proportional to the inverse of the Fresnel number. One transverse dimension is considered, sufficient to display the appearance of sidebands. The temporal evolution of Q is approximated by a relaxation equation of the form[4]

$$\tau\partial_t Q + \eta Q = \Gamma\frac{A_1 A_2{}^*}{|A_1|^2 + |A_2|^2}\,, \tag{2}$$

where τ is the relaxation time, $\eta = (E_D + E_q + iE_0)/(E_\mu + E_D + iE_0)$ is a parameter dependent on the internal electric fields of the crystal, and $\Gamma = \Gamma_0(1 + E_q/E_D)(E_D + iE_0)/(E_\mu + E_D + iE_0)$ is the PR coupling constant. E_0 is the external dc field, applied to the crystal along the propagation direction z. The Kukhtarev model, which will be modified to accommodate the nonlinear modulation-depth dependence, is adopted. It is also assumed that the characteristic transverse length over which Q changes is large compared with the grating period.

Modulation-depth effects are accounted for phenomenologically, by assuming that the coupling constant Γ_0 is a function of the modulation depth m. Such a procedure is well documented in the literature.[5] For the model function we pick one of the forms used, known to improve the agreement with experiment:

$$\Gamma_0(m) = \frac{\Gamma_0}{1 + bm/2}\,, \tag{3}$$

where b is a fitting parameter. Rigorous inclusion of modulation-depth effects requires numerical solution of the Kukhtarev material equations,[5] together with the solution of wave equations. This is computationally expensive.

The stability analysis proceeds with the assumption of a small perturbation of the wave and the grating amplitudes:

$$A_1(z, x, t) = A_1^0(z)[1 + \epsilon a_1(z, x, t)]\,, \tag{4a}$$

$$A_2(z, x, t) = A_2^0(z)[1 + \epsilon a_2(z, x, t)]\,, \tag{4b}$$

$$Q(z, x, t) = Q^0(z)[1 + \epsilon q(z, x, t)]\,, \tag{4c}$$

about an unperturbed plane-wave state, denoted by the superscript 0. Substituting Eqs. (4) into Eqs. (1) and (2) and performing the Laplace transform in t and

0146-9592/97/080498-03$10.00/0

the Fourier transform in x, one obtains the following equations for the perturbation components:

$$\partial_z a_1 - i\phi k^2 a_1 = \Gamma_e \frac{a_1 - a_2 - q}{1 + r + b\sqrt{r}}, \tag{5a}$$

$$-\partial_z a_2 - i\phi k^2 a_2 = \Gamma_e^* \frac{r(a_1 - a_2 + q^*)}{1 + r + b\sqrt{r}}, \tag{5b}$$

$$(\tau_e\lambda + 1)q = \frac{a_1 - a_2 - r(a_1 - a_2)^* + b\sqrt{r}(a_1 - a_2 - a_1^* + a_2^*)/2}{1 + r + b\sqrt{r}} \tag{5c}$$

of the order of ϵ. Here $r(z) = I_1^0(z)/I_2^0(z)$ is the unperturbed beam ratio at some point z in the crystal, and $\Gamma_e = \Gamma/\eta$ and $\tau_e = \tau/\eta$ are the effective complex coupling and relaxation constants. The modulation depth is included in Eqs. (5) through the dependence on r: $m = 2\sqrt{r}/(1 + r)$.

Equation (5c) is an algebraic expression for q that can be substituted into Eqs. (5a) and (5b). They are now cast in a matrix form,

$$\partial_z \mathbf{a} = \mathcal{A}(z, k, \lambda)\mathbf{a}(z, k, \lambda), \tag{6}$$

where $\mathbf{a} = (a_1, a_1^*, a_2, a_2^*)^T$. This equation cannot be solved analytically. However, the ratio of beams r is roughly constant for reflection gratings. An approximation of $r = 1$ is quite good for strong couplings and a weak incident backward beam. This means that $m = 1$ but does not lead to an inconsistency, since strong modulation depth effects are accounted for. Then the solution of Eq. (6) is given by $\mathbf{a}(L) = \mathcal{F}(L)\mathbf{a}(0)$, where $\mathcal{F}(z) = \exp(\mathcal{A}z)$ is the flow matrix of the linearized system and L is the thickness of the crystal. The flow matrix consists of four 2×2 blocks $\mathcal{F}_{ij}(i, j = 1, 2)$. Taking into account two-point boundary conditions, we obtain the final form of the solution,

$$\mathbf{a}(z_{\text{out}}) = S(k, \lambda)\mathbf{a}(z_{\text{in}}), \tag{7}$$

where S is the scattering matrix of the problem and z_{out} and z_{in} are the output and the input faces of the crystal for the respective beams.

The poles of the scattering matrix determine the nature and the dynamics of an instability. In our case, the poles of S are found from the equation $\det(\mathcal{F}_{22}) = 0$, which, when written explicitly, leads to the following dispersion relation:

$$\exp(\gamma) + \exp(g) + 2\exp\left(\frac{\gamma + g}{2}\right) \times [\cos(\chi_1)\cos(\chi_2) + p\,\mathrm{sinc}(\chi_1)\mathrm{sinc}(\chi_2)] = 0, \tag{8}$$

where ${\chi_1}^2 = \kappa(\kappa + \beta) - \gamma^2/4$, ${\chi_2}^2(\lambda) = \kappa(\kappa + h) - g^2/4$, and $p(\lambda) = \kappa[\kappa + (\beta + h)/2] + \beta h/2 + \gamma g/4$. The functions $g(\lambda) = \lambda[\Gamma_e\tau_e/(\lambda\tau_e + 1) + (\Gamma_e\tau_e)^*/(\lambda\tau_e^* + 1)]/2$ and $h(\lambda) = \lambda[\Gamma_e\tau_e/(\lambda\tau_e + 1) - (\Gamma_e\tau_e)^*/(\lambda\tau_e^* + 1)]/2i$ appear because of the variations in Q. γ and β are, respectively, the real and the imaginary parts of Γ_e, and $\kappa = \phi k^2$. Equation (8) is one of the main results of this Letter. It is written for $b = 0$, so that it can be compared directly with the other[2,3] published results. Let us analyze its consequences.

The instability threshold is inferred from the lowest-lying branches of the dispersion relation (Fig. 1). The generic feature of transverse instabilities, as found here, is that they arise at a finite value of E_0 through a Hopf bifurcation of the fixed point (unperturbed solution) at a characteristic transverse wave vector k and a characteristic frequency $\Omega = \mathrm{Im}\,\lambda$. The

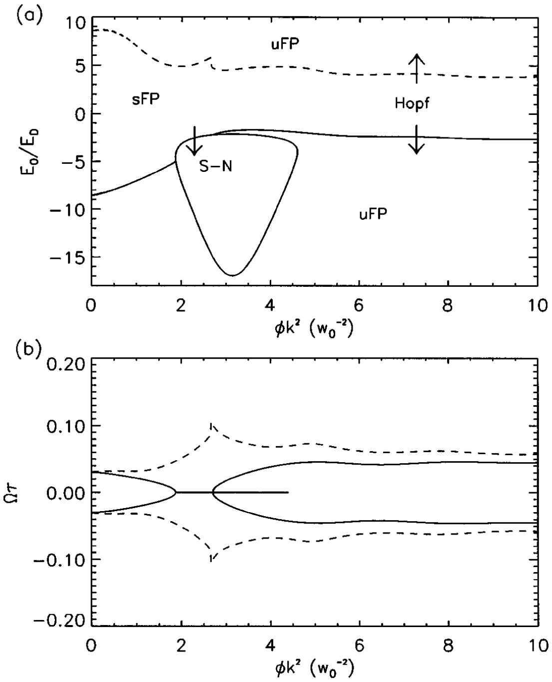

Fig. 1. (a) Threshold curves of the applied electric field and (b) threshold frequency of the grating amplitude as functions of the transverse wave vector. The solid curves are for $E_0 < 0$; the dashed curves for $E_0 > 0$. The beam ratio inside the crystal is $r = 1$, the bare coupling constant is $\Gamma_0 = 2\ \text{cm}^{-1}$, and $b = 0$. sFP and uFP denote the regions of stable and unstable fixed points, respectively. Hopf and S-N (saddle node) indicate the nature of the bifurcation as the threshold curve is crossed in the direction of the arrows.

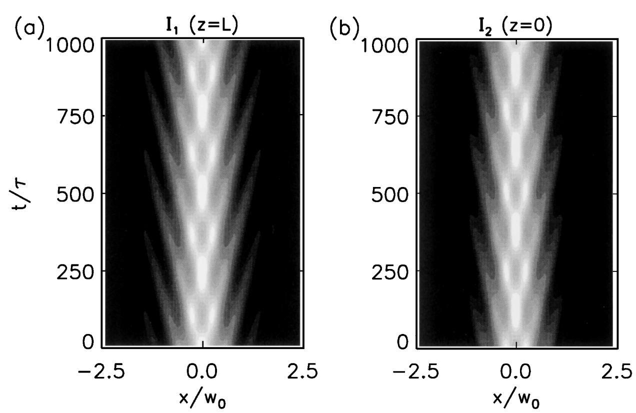

Fig. 2. Running transverse waves obtained in a numerical simulation above the instability threshold. Transverse output distributions of (a) I_1 and (b) I_2 are shown as functions of time, after transients have died away. The parameters of the simulation are the same as in Fig. 1. The input beam ratio is $r^0 = 20.09$ (corresponding to $r = 1$). Other parameters are $E_0 = -2E_D$ and $\phi = 0.001$. E_0 is chosen somewhat above $E_0^c \approx -1.7E_D$ to avoid critical slowing down.

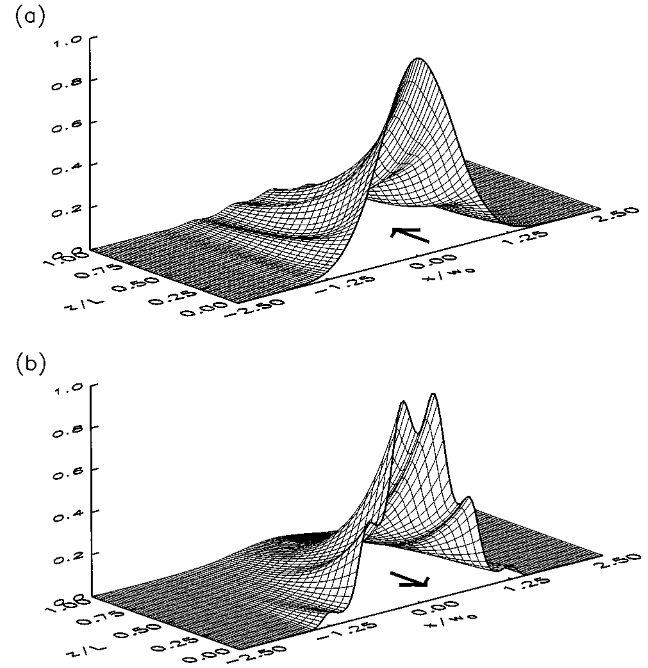

Fig. 3. Spatial distribution of intensities (a) I_1 and (b) I_2 within the crystal at time $t = 1000\tau$. The arrows indicate the propagation direction. The parameters are the same as in Fig. 2.

minimum value of k at which the instability occurs (which translates into a critical angle at which the sidebands appear in the far field) is found at the point where Re λ becomes positive for the first time. These results differ from those previously published[2,3] in two important aspects. The first is that the plane-wave limit is predicted to be unstable for both polarities of E_0, with the critical value approximately equal to ± 8.6 diffusion fields E_D of the crystal. This agrees with earlier accounts,[6] in which a four–wave mixing process in the plane-wave approximation was driven to instabilities and temporal chaos through a series of Hopf bifurcations.

The second aspect is the importance of the sluggishness of PR media, which at a threshold (either in E_0 or in Γ_0) causes slow oscillation of the grating amplitude. This oscillation implants a small frequency offset in the counterpropagating beams and drives them to instability. The frequency shift introduced by Saffman *et al.*[2] is of a different nature. The consequence of not including variations in Q is that instability balloons appear in the threshold curves. A similar balloon is part of what is displayed in Fig. 1. The characteristic frequencies where the balloons appear are zero. Hence the nature of the bifurcation as the balloon border is crossed changes to that of a saddle node. However, this happens at a threshold that is always higher than the one obtained for the Hopf bifurcation and therefore is not observable. Here the lowest (actually, the highest, for negative E_0) threshold of the applied field $E_0^c \approx -1.7E_D$ is attained at $\phi k^2 \approx 3.6{w_0}^{-2}$, where w_0 is the beam spot size. The corresponding $\Omega^c \approx 0.031\tau^{-1}$.

To corroborate these findings, we produce a reliable numerical code based on the modified beam propagation method[4] that treats the transverse two-wave mixing in reflection geometry and reveals the instabilities according to the model. The agreement is pronounced, both qualitatively and quantitatively. Figure 2 depicts running transverse waves slightly above the predicted threshold, obtained as a result of spontaneous destabilization of two Gaussian beams incident upon the opposite faces fo the crystal. Figure 3 displays the spatial distribution of the fields within the crystal at some instant of time. If the polarity of E_0 is flipped (keeping other parameters unchanged), then no instability is found, in agreement with the stability analysis. The value of $E_0 = +2E_D$ is below the predicted threshold of $E_0^c \approx +3.2E_D$.

Research at the Institute of Applied Physics is supported within the Sonderforschungsbereich 185 Nichtlineare Dynamik of the Deutsche Forschungsgemeinschaft. Research at the Institute of Physics is supported by the Ministry of Science and Technology of the Republic of Serbia. We give special thanks to M. Münkel for many fruitful discussions.

References

1. T. Honda, Opt. Lett. **18,** 598 (1993).
2. M. Saffman, A. A. Zozulya, and D. Z. Anderson, J. Opt. Soc. Am. B **11,** 1409 (1994).
3. B. Sturman and A. Chernykh, J. Opt. Soc. Am. B **12,** 1384 (1995); T. Honda and P. P. Banerjee, Opt. Lett. **21,** 779 (1996).
4. M. R. Belić, J. Leonardy, D. Timotijević, and F. Kaiser, J. Opt. Soc. Am. B **12,** 1602 (1995).
5. P. Réfrégier, L. Solymar, H. Rajbenbach, and J.-P. Huignard, J. Appl. Phys. **58,** 45 (1985); C. H. Kwak, S. Y. Park, J. S. Jeong, H. H. Suh, and E. H. Lee, Opt. Commun. **105,** 353 (1994).
6. W. Krolikowski, M. Belić, M. Cronin-Golomb, and A. Bledowski, J. Opt. Soc. Am. B **7,** 1204 (1990).